energies

MDPI

Article

An Experimental Study on the Quantitative and Qualitative Characteristics of Tar Formed during Ex Situ Coal Gasification

Marian Wiatowski

Główny Instytut Górnictwa (Central Mining Institute), Plac Gwarków 1, 40-166 Katowice, Poland; mwiatowski@gig.eu

Abstract: Over the three-day gasification test of a large coal block with oxygen in atmospheric pressure conditions, the yield and composition of the tar collected was investigated. The tar was sampled approximately every 7 h into sorption tubes directly from the reactor outlet. Sand, with a moisture content of 11%, was used as an insulating material to simulate the environment of the gasified coal seam. Light aromatic hydrocarbons (BTEX), phenols, and polycyclic aromatic hydrocarbons (PAHs) were determined in the tar. The results that were obtained were recalculated into the concentrations of the individual components of the tar and its mass stream in the process gas. The residence time of the tar in the reactor, its molar mass, and the H/C ratio were also calculated. As the reaction progressed, the water that was contained in the wet sand started to react with the gasified coal, which significantly affected the composition and amount of the obtained process gas and the produced tar. Due to an increase in the amount of generated gases and steam, the residence time of the tar vapours in the reactor decreased as the gasification progressed, ranging from approximately 1 s at the beginning of the process to 0.35 s at the end. The obtained tar was characterised by a high average content of BTEX fractions at approximately 82.6%, PAHs at 14.7%, and phenols at 2.7%. Benzene was the dominant BTEX compound, with a concentration of 83.7%. The high content of the BTEX compounds, especially benzene, was a result of secondary processes taking place in the tar (hydrocracking and steam reforming), and as a result of which, in the presence of hydrogen and steam, the heavier components of the tar were transformed into lighter ones. The total yield of the tar from this UCG (underground coal gasification) process—calculated per 1 ton of gasified coal—was 1.8% (counted on the basis of the analysed tar composition). Comparing this result to the efficiency of the classic coking process, the tar yield was about three times lower.

Keywords: underground coal gasification; UCG; tar; BTEX; PAHs; phenols

Citation: Wiatowski, M. An Experimental Study on the Quantitative and Qualitative Characteristics of Tar Formed during Ex Situ Coal Gasification. *Energies* **2023**, *16*, 2777. https://doi.org/10.3390/en16062777

Academic Editors: Ján Kačur, Milan Durdán and Marek Laciak

Received: 3 February 2023
Revised: 14 March 2023
Accepted: 14 March 2023
Published: 16 March 2023

1. Introduction

The underground coal gasification (UCG) process consists of the reaction of underground coal with gasifying agents such as oxygen, air, and/or steam, which, at high temperatures, results in a gas containing mainly hydrogen, carbon monoxide, carbon dioxide, and methane. In addition, this gas also contains smaller amounts of ethane, hydrogen sulfide, water, and tar [1,2]. If the gasification is carried out using air or oxygen-enriched air, then the gas also contains nitrogen. This resulting gas is transported by a pipeline to the surface, where, after cleaning, it can be used for energy generation or as a raw material in the chemical industry. Although the UCG process is rather well documented in the literature [3–5], there is little information about the tar produced by this technology. This is because the main goal of this process is to obtain a gas with the highest possible calorific value, and tar is a byproduct [6]. The most important parameter that affects the course of tar production is the gasification temperature [7]. When the temperature is increased to 350 °C, volatile substances, such as steam and adsorbed gases, are released from the gasified coal seam as a result of evaporation (not thermal decomposition). The temperature range of 350–750 °C is the main area of decomposition for the coal components, in which

the largest amount of tar is emitted, with the most intensive production of the tar occurring at temperatures of approximately 600 °C [8]. At temperatures above 1000 °C, tar is no longer emitted, but due to secondary processes occurring in the previously released tar (cracking and aromatization), its composition changes. As the UCG process progresses, an increasing amount of the coal is gasified, and depending on the scale of the test, some amounts of tar are almost always present in the process gas [9].

In the UCG process, the participation of water is necessary. At high temperatures in the reactor, the water is transformed into steam, which reacts with the coal and produces water gas (CO + H_2). These reactions can be described by the equations:

$$C + H_2O \rightarrow CO + H_2 \quad \Delta H = +135.7\ kJ/mol \tag{1}$$

In the case of excess steam, a second process takes place in parallel:

$$CO + H_2O \rightarrow CO_2 + H_2 \quad \Delta H = -33.2\ kJ/mol \tag{2}$$

The reaction described by Equation (1), which produces both carbon monoxide and hydrogen, is one of the most important reactions within coal gasification. It is endothermic and reversible. It requires heat energy, and is favoured by high temperature and rather low pressure, with the temperature not having as great an influence as the pressure. Above 800 °C, the equilibrium gas concentrations (steam, carbon monoxide, and hydrogen) do not change significantly [10,11]. The optimum parameters for this reaction are a temperature of 700–900 °C and a pressure of 3–4 MPa [12]. Reaction (2), called a shift conversion or a water–gas shift reaction, is a reversible, moderately exothermic reaction, a result of which is that the amount of hydrogen that is produced in the gases increases compared to that of the carbon monoxide [10,13]. The direction of reaction (2) strongly depends on the conditions in the reactor. If the temperature is too high, the reverse reaction occurs, and the amount of carbon monoxide increases at the expense of hydrogen. Since there is no volume change in this reaction, the pressure has no effect on the hydrogen yield. The typical parameters of this reaction are a temperature of 200–500 °C and a pressure of 0.3–4 MPa [13].

The water that takes part in the gasification process can influence the composition and quantity of the tar obtained. In one study [14], it was found that the presence of water vapour increases the rate of the decomposition of the heavier components of the tar (cracking), resulting in an increase in the yield and a decrease in the molecular weight. Further studies of this effect [15] have shown that, as a result of reaction (1), the original macromolecular structure of the coal surface is disrupted, thus opening the pores of the coal [16], through which the tar components escape as a result of increased permeability. As a result of this reaction, the yield of the tar increases [17]. The hydrogen that is produced can build into the separated tar substances (reforming) and inhibit the repolymerisation reaction of the molecules. As a result of these reactions, the amount of separated tar with a lighter character increases. On the other hand, when too much water participates in the UCG process, the average pyrolysis temperature decreases, and the aforementioned effect is weakened [18,19].

An example of a pyrolysis reaction can be the thermal decomposition of toluene. It is a radical process that can be described by the following reactions (3) and (4):

$$C_6H_5CH_3 + H^{\cdot} \rightarrow C_6H_6 + CH_3^{\cdot} \tag{3}$$

$$H_3^{\cdot} + H^{\cdot} \rightarrow CH_4 \tag{4}$$

As a result of this reaction, at a high temperature of approximately 1000 °C and in the presence of hydrogen, toluene decomposes to benzene and methane [20]. If another alkylbenzene, such as ethylbenzene, is thermally decomposed, ethane can be formed

instead of methane. Ethane can also be formed by the termination of two methyl radicals that collide with each other. This is described by reaction (5):

$$\dot{CH_3} + \dot{CH_3} \rightarrow C_2H_6 \quad (5)$$

Under the conditions in the reactor during gasification, the source of the hydrogen radicals can be hydrogen or steam. According to other studies [21], at the high temperatures that prevail in the reactor (800–1000 °C), in the presence of steam, the reforming of tar to carbon monoxide and hydrogen can also occur. This is represented by Equation (6):

$$C_nH_m(\text{tar}) + nH_2O \rightarrow nCO + (n + m/2)H_2 \quad (6)$$

As a result of this reaction, the amount of the tar that is formed decreases, and the concentration of the carbon monoxide and hydrogen in the process gas increases. This reaction is favoured [22] by the presence of a catalyst (Al, Ni). Another factor determining the yield and composition of the tar is its residence time in the reactor. A shorter residence time favours fewer partial cracking events over time, and consequently, the overall tar yield is increased. With longer residence times, the opposite can be expected. For example, more than 80% of the tar can decompose within seconds in the pyrolysis process at 1000 °C [23]. This tendency is also visible in the data on surface syngas and related tar yields [24].

Numerical simulation, in addition to the experiments, can also be effectively applied to the study of tar formation and conversion in UCG. In work [25], the UCG process was simulated on the basis of the American Hanna I and Centralia PSC tests [26,27]. The model results for the tar show that the trends of the changes in its performance are at an acceptable level in relation to the values from the reference field tests. The authors of the paper admit, however, that, due to the simplified assumptions of the model, the tar yield was significantly overstated in relation to the actual values. Accurate results were obtained in the improved model [28]. The quantitative effect of the tar yield varied from a few percent to more than 50% compared to the specified actual cases. More information on these models can be found in the dissertation [29].

The tar contained in the process gas stream (vapours and/or aerosol) is condensed as a result of lowering the temperature of the gas during transport through the outlet pipeline to the surface. Its heavier components condense in the higher temperature zone, while its lighter components condense in places closer to the surface, where the temperature is lower. This phenomenon negatively affects the course of the gas transport to the surface, because the condensing tar reduces the cross-section of the pipeline transporting the process gas [30–36]. In extreme cases, a clogged pipeline may occur. The described phenomena can be partially prevented by the appropriate temperature control of the gasification process. If the outlet gas temperature is high, the tar will condense to a lesser extent in the underground part, but more intensively on the surface. This will result in higher tar yields, and will necessitate the expansion and further utilisation of tar–gas separation equipment. It should be noted that, if the gas cleaning system is not equipped with an efficient recovery system, contained in the tar's light aromatic hydrocarbons (BTEX), even at room temperature, may not condense due to their high volatility and will remain in the process gas. For example, during in situ tests [37,38] in tar that condensed on the surface at the temperature of 20–40 °C, no presence of the BTEX compounds was found, while the measurement of their direct presence in the process gas showed their high content [9]. More detailed analyzes have shown that even volatile tar components can remain in areas closer to the reactor (hot zones) by dissolving into previously condensed heavier tar components [30]. The amount of tar produced in the process depends on the conditions of the process and can be different in each experiment. In Poland, during two UCG tests at the "Barbara" mine and a third at the "Wieczorek" mine, the tar yields were 0.23%, 0.06%, and 0.91% of the mass of the gasified raw coal, respectively [38,39]. However, most data on the yields of the tar obtained from large-scale in situ gasifications come from Russian and US tests. Thus, based on a series of tests at the Podzemgaz South Abinsk Station [40], the tar yield

was approximately 0.15–0.20% of the mass of gasified coal. Comparing these data with the 2–5% tar yield that is obtained in a typical coal coking process, Pavlovich and Strakhov [40] found that the tar yield from the UCG process is 13–25 times lower. The data from the American UCG tests [41–43] showed that the yield of the tar was slightly higher than those of the Russian tests. In these tests, the yield of the tar (referred to as oil condensates) from the raw coal was approximately 1–3% of the weight of the gasified coal (e.g., 1.6% of the weight of the carbon for Rocky Mountain 1; 1.9% of the weight of the carbon for Hanna IV; and 1.9% of the weight of the carbon in Hanna II Phase III). Based on these data, Camp and White [41] concluded that, compared with the tar yields of a typical coal coking process, a significant part (approximately 80%) of the tar products that were produced by the underground coal gasification process underwent secondary reactions or condensation and remained underground. It should be noted that these conclusions resulted from measuring the amount of the tar obtained after the process gas had passed from the underground reactor to the surface, and assuming that the total (lossless) amount of the tar obtained from the UCG process was similar to the tar yield of a typical coal coking process. This assumption should be tested experimentally, because the UCG process differs from coal coking in many of its process parameters. One of the most important differences is that, to obtain a sufficiently high temperature inside the reactor, part of the coal is burned, and with it, a certain amount of the produced tar. This is confirmed by the literature data on earlier UCG tests, which show that only 75% of the coal is converted to gas and 25% is converted to ash, water, and tar [44]. Therefore, the amount and properties of the tar obtained from the UCG process will differ from those of the coal coking process. Detailed data on the quantity and composition of the tar obtained from the UCG process could be obtained from the measurements of the tar samples taken directly from the reactor outlet, however, there are not many such works in the available literature. This is because of technical and safety reasons. Such measurements in real conditions are rather impossible; however, in ex situ conditions, measurement is more realistic.

In three such studies, carried out on small coal blocks [45–47], changes in the composition of the tar collected directly from the interior and outlet of the reactor were investigated during an ex situ coal gasification. On the basis of the work [45], it was found, among others, that in comparison to the tar from the reaction zone, the tar from the reactor outlet, due to cracking and condensation, contained a smaller amount of heavier substances. The results of the tar tests in study [46] showed that when the coal was gasified with oxygen, the amount of the tar obtained at the reactor outlet was greater than that in the case of using air, and that an increase in the oxygen flow rate caused an increase in the amount of the obtained tar.

In another paper [47], tar samples were taken from three places: two from the inside of the reactor and the third from the outlet. The analysis of the composition of the tars concerned only a few selected components that were present in the highest concentrations. It was found that the most abundant component of all the tars was the compound $C_{15}H_{13}N$ and its isomers. Compared with the tar taken from the upper part of the reactor, the tar taken from the lower part was characterized by a lower content of PAHs and a lower boiling point. The authors of the work stated that this was due to the decomposition of the heavy tar components, as a result of the temperature increase in the reaction zone.

However, in the mentioned three papers [45–47] no tar yield calculations were performed. The presented literature review shows that there are very few detailed data on the amount and composition of the tar taken directly from the reactor outlet during the UCG process. Furthermore, the simulations of the tar yield and composition, due to the high degrees of complexity and unpredictability of the phenomena occurring during the UCG process, are not accurate enough. Therefore, an innovative approach to achieving the research goal in this area was to determine the efficiency of the individual tar components (single and in groups) and the average residence time of the tar vapours in the reactor, on the basis of the measurements made directly from the reactor outlet. In addition, the effect

of the gasification time on the tar composition was analysed, the H/C ratio in the tar was determined, and the average molecular weight of the tar was calculated.

To perform such measurements, a previously conducted ex situ experiment [48] used the oxygen gasification of a large block of hard coal. The experiment investigated, among other things, the effect of siderite addition on the UCG process, and an attempt was made to determine the temperature distribution in the reactor. During the same experiment, the tar was sampled directly from the reactor outlet and analysed qualitatively and quantitatively. The results contributed to an understanding of the quantity and composition of the tar obtained in the real UCG process, which can help in designing plants to carry out this process on a large scale.

2. Experimental

2.1. Description of Installation for the Ex Situ UCG

A scheme of an installation for ex situ coal gasification under surface conditions is shown in Figure 1, while details of the reactor construction are shown in Figure 2a–c. The actual view of the UCG reactor for ex situ tests is shown in Figure 3.

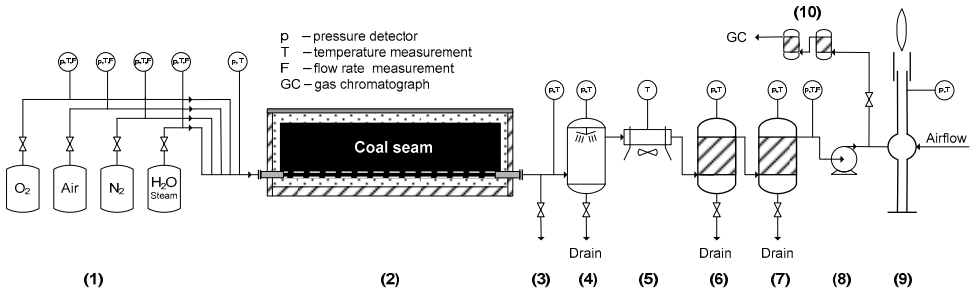

Figure 1. Scheme of the ex situ UCG installation [48]: (1) reagent supply system, (2) gasification reactor, (3) connection for tar sampling, (4) water scrubber, (5) air cooler for process gas, (6,7) gas separators, (8) centrifugal suction fan, (9) thermal combustor, and (10) gas purification module for GC analysis.

The main element of this installation is a reactor in which gasification can be carried out in a simulated coal seam, with a maximum length of 7.0 m and a cross-section of 1.0 × 1.0 m. This reactor enables coal gasification at temperatures of up to 1600 °C and an overpressure of no more than 0.5 bar. The gasifying agent can be oxygen, air, water vapour, or mixtures of these gases. Nitrogen is used for inerting the installation and for cooling the reactor after the gasification process is complete. To quickly remove the volatile gasification products from the reaction zone, the installation is equipped with a suction fan (Figure 1). By reducing the residence time of the volatile products in the reactor, the risk of a partial combustion of the flammable components of the process gas in the oxygen stream is reduced, and the possibility of secondary reactions in the produced tar is limited. To prevent the air from being sucked into the reactor by the suction fan, the gasification process is carried out with a minimum overpressure of 5–10 hPa. The pressure sensors are located at the inlet and outlet of the reactor, and in the wet scrubber. The hot process gas coming out of the reactor passes through a scrubber, inside of which, water is sprayed. This quickly cools the gas and removes the tar. The further purification of the gas takes place after the gas passes through the air cooler, separators of moisture, oil–tar substances, and solid particles. The cleaned gas is utilised by burning it in a thermal combustor. Before this combustion, part of the gas stream is taken for a chemical analysis, where the concentrations of hydrogen, carbon monoxide, carbon dioxide, methane, ethane, and hydrogen sulfide are determined with a gas chromatograph. The arrangement of the thermocouples in the reactor is shown in Figure 2a,c. The white circles that are shown in Figure 2a indicate the places that are constructively designed for the thermocouples, while the numbers next to the circles indicate the thermocouples that were actually used in this process (18 thermocouples). The first row of the thermocouples (T2–T5) was located

at the level of the fire channel, at a distance of 0.2 m from the bottom of the reactor. The second and third rows of the thermocouples (T8–T14 and T15–T21) were located higher up, at every 0.25 m increment. Thermocouple T1, which was located closest to the oxygen inlet, had to be removed due to its unfavourable placement relative to the feed pipe. The pressure in the system was measured at the reactor inlet and outlet, as well as in the gas treatment and transport system for utilisation. The control and measurement apparatus recorded all the plant operation data every 10 s. The obtained results were recalculated to standard conditions (T = 273.15 K, p = 1013.25 hPa).

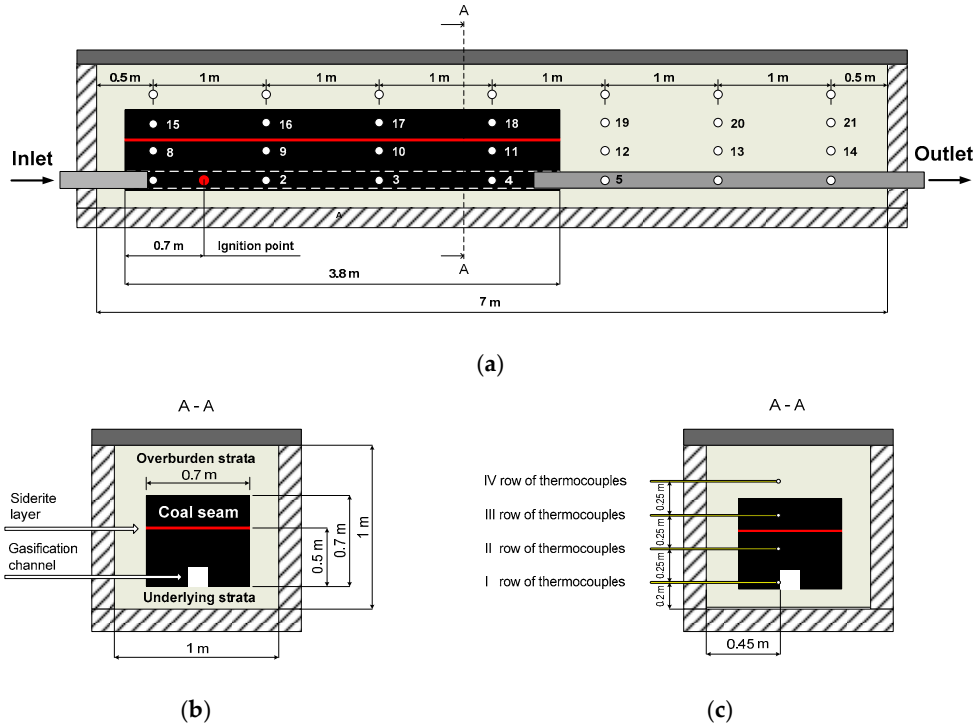

Figure 2. Details of the reactor construction [48]: (**a**) longitudinal cross-section—arrangement of coal seam and thermocouples position, (**b**,**c**) cross-section: dimensions of the coal seam and thermocouples distances.

Figure 3. Photo of a prepared ex situ UCG reactor, operating at atmospheric pressure.

2.2. Preparation of a Coal Sample and Siderite Interlayer

The coal that was subjected to gasification came from the Piast mine, located in the south of Poland (Upper Silesian region). The dimensions of the gasified coal block were 3.8 × 0.7 × 0.7 m (width, depth, and height). The upper part of the block of coal was cut horizontally at a height of 0.5 m, and a 2 cm thick layer of siderite was placed at the intersection. In the lower part of the block of coal, a fire channel with a cross-section of 0.1 × 0.1 m was cut out along its entire length. The gasification agent was supplied on one side of the channel, and the gaseous gasification products were led outside on the other side. The prepared coal block was placed inside the reactor on a 0.2 m thick wet sand layer. The free space between the coal block and the reactor side walls was also filled with wet sand. The sand was used as an insulating material, simulating moisture in the vicinity of the gasified coal seam. The weights of the coal, siderite, and wet sand that were used were 2300 kg, 150 kg, and 7900 kg, respectively.

2.3. Methods of Measuring the Properties of Gaseous Media

- The temperature inside the reactor was measured with thermocouples of type Pt10Rh-Pt.
- At the reactor inlet, outlet, and in the scrubber, Pt100 resistance sensors were used.
- The pressure was measured by WIKA digital transmitters of type IS-20-S.
- The process gas flow was measured with an ELSTER bellows gasometer of type BK-G10M.
- The gas composition was measured using an Agilent 3000A gas chromatograph.
- The flow of the oxygen was controlled by the Bronkhorst EL-FLOW mass flow controller, model F-202AV-M20-RAD.

2.4. The Course of the Experiment

A description of the gasification stages is presented in Table 1.

Table 1. Stages of the UCG test.

Stage No.	Stage Description	Gasification Agent	Flow Rate (m^3/h)	Time Interval (h)	Duration (h)
1	Coal ignition and gasification process	Oxygen	4.5	0–72	72
2	Extinguishing and cooling down of reactor	Nitrogen	2	72–144	72

The coal gasifying agent was 99% pure oxygen taken from a cylinder bundle. Upon starting the experiment, the suction fan was first activated, and then the coal seam was ignited with a pyrotechnic charge [49]. The incendiary charge was placed 0.7 m from the beginning of the coal block. The generated temperature during the 3–5 min of the burning of the charge was 800–900 °C. The ignition process was started with an oxygen flow rate of 2 m^3/h. After igniting the coal, the oxygen flow rate increased to 4 m^3/h. The process continued until the oxygen concentration in the process gas decreased to a value of less than 1%. At this point in time, the oxygen flow rate increased to 4.5 m^3/h, and this value was kept constant throughout the experiment. At the same time, together with the ignition of the coal seam, a pump was activated that fed water to the wet scrubber (water injection 14 kg/h). This was done to prevent the liquefied tar from clogging the pipeline that transports the process gas. After 72 h, the oxygen supply was stopped and the reactor was cooled down with a stream of nitrogen. The nitrogen flow rate was selected experimentally. Using a nitrogen flow of 2 m^3/h, the cooling time to the ambient temperature (20 °C) was approximately one week, while with a flow of 4 m^3/h, the cooling time was approximately two days shorter. A flow of 2 m^3/h was therefore chosen. This nitrogen stream provided sufficient reactor inertization, low nitrogen consumption, and an acceptable cooling rate. During the test, the flow and composition of the produced gas were

analysed every hour. Every two hours, the wet scrubber was emptied, and the amount of the obtained postprocessing water was weighed.

2.5. Method of Tar Sampling and Analysis

The tar samples were taken every few hours (6–8 h), directly from the process gas, through the tar sampling connection (Figure 1). In total, ten samples of the tar were collected. The tar sampling point was intentionally designed to be close to the reactor outlet (at a distance of approximately 50 cm) to minimise the occurrence of secondary reactions related to the long residence time of the tar at high temperatures. Small volumes of gas, amounting to a few dm^3, were sucked in with a type SKC aspirator, Model 224-PCMTX8, and then passed through selected fixed-bed sorption tubes. For the analysis of the light monoaromatic hydrocarbons, such as benzene, toluene, ethylbenzene, and xylenes (BTEX), polycyclic aromatic hydrocarbons (PAHs), and phenolic compounds, sorption tubes with charcoal (SKC Inc., Eighty Four, PA, USA, Anasorb CSC), porous hydrophobic organic polymer (SKC Inc., XAD-2), and silica gel (SKC Inc., Silica Gel) were used, respectively. Each sampling was preceded by purging the sampling system with fresh process gas. The samples that were collected represent the part of the tar that left the reactor with the process gas, i.e., the non-condensable parts of the coal gasification product and/or their aerosols. The list of the samples that were collected is presented in Table 2.

Table 2. List of the tar samples for analysis.

Sample No.	Time of Gasification (h)	Time Interval between Collected Samples (h)
1	6	6
2	13	7
3	20	7
4	27	7
5	34	7
6	41	7
7	48	7
8	55	7
9	62	8
10	71	8

The first step of the analysis was to extract the BTEX, PAHs, and phenolic components from the sorption tubes, using the solvents carbon disulfide, cyclohexane, and acetone, respectively. The samples were then shaken, filtered, and analysed on a capillary column with an AGILENT Technologies 7890A gas chromatograph. A flame ionisation detector (FID) was used to analyse the BTEX compounds and phenols, while a chromatograph coupled with an Agilent 5975C mass spectrometer in Selected Ion Mode (SIM) were used to detect the PAH compounds.

3. Results

3.1. Results of the Analysis of Coal, Siderite, and Moisture Content in Sand

The analysis of the coal and sand was carried out in the certified laboratory at Silesian Technical University, according to Polish standards. The obtained results of the technical and elemental analysis of the coal are shown in Table 3.

The analysed bituminous coal was characterised by a low moisture content (as received) of 4.7%, a relatively high ash content of 16.30%, and a volatile matter content of 30.10%. Its calorific value was 22.719 MJ/kg. The moisture content in the sand, determined in accordance with the PN-G-04511:1980 standard, was 11.0%. The high humidity of the sand was as a result of storing it in an open space, which exposed it to the effects of weather conditions, including rain. The analysis of the siderite was carried out at the Silesian Interdisciplinary Education and Research Centre in Chorzów. Its elemental composition was determined by X-ray fluorescence (XRF) from a ZSX Primus II Rigaku spectrometer, and the

results were recalculated into oxides. Its CO_2 content was determined by the volumetric method in a Scheibler-Dietrich apparatus. The data that were obtained show that iron oxide is the dominant component, at 41.08% FeO. The content of the other minerals was lower, at 10.72% silicon dioxide, 5.03% aluminium trioxide, 3.33% magnesium oxide, and 2.37% calcium oxide, with a measurement accuracy of up to 1 wt.%. The CO_2 content ranged from 33.1 to 35.7% by weight, with an average of 34.6%.

Table 3. Proximate and ultimate characteristics of the coal from the Piast mine and standard analytical methods [48].

Parameter	Symbol	Unit	Value	Standard [b]
As received				
Total moisture	W_t^r	(%)	4.70	PN-G-04511:1980
Ash	A_t^r	(%)	16.30	PN-G-04560:1998
Volatiles matter	V_r^a	(%)	30.10	PN-G-04516:1998
S total	S_t^r	(%)	0.83	PN-G-04584:2001
Lower heating value	Q^r	(kJ/kg)	22,719	PN-G-04513:1981
Analytical				
Moisture	W^a	(%)	2.95	PN-G-04560:1998
Ash	A^a	(%)	16.60	PN-G-04560:1998
Volatiles matter	V^a	(%)	30.65	PN-G-04516:1998
Lower heating value	Q^a	(kJ/kg)	23,137	PN-G-04513:1981
S_t^a total		(%)	0.85	PN-G-04584:2001
C^a		(%)	62.50	PN-G-04571:1998
H^a		(%)	4.39	PN-G-04571:1998
N^a		(%)	1.04	PN-G-04571:1998
O^a *		(%)	11.67	

r—as received, t—total, a—analytical, and b—Polish testing by the accredited laboratory. * Oxygen calculated as: $(O^a) = 100 - (W^a) - (A^a) - (C^a) - (H^a) - (S_t^a) - (N^a)$.

3.2. Temperature Distribution

The temperatures in row I of the thermocouples (fire channel) and row II of the thermocouples, as well as the temperatures at the reactor outlet and inside the wet scrubber, are shown in Figure 4a–c. Figure 4a shows that the highest temperatures in the fire channel, approximately 1200 °C, were indicated by the T2 thermocouple, which was located approximately 1 m from the beginning of the coal seam. The lowest temperatures of 350 °C were recorded by the furthest thermocouple T4. Thermocouple T5, which was placed outside of the block of coal, showed maximum temperatures that did not exceed 330 °C. The temperatures in the second row of the thermocouples were similar to those in the first row. Figure 4a shows that the temperatures in the fire channel decreased with increasing distance from the place of ignition. In row II, there was a similar relationship, with the exception of the T9 thermocouple, which indicated higher values than thermocouple T8, because thermocouple T9 was located directly above the ignition point of the coal seam. All the thermocouples recorded temperature fluctuations that occurred at similar time intervals. The most characteristic interval was between 24 and 32 h.

The temperature measurement point of the process gas at the reactor outlet was located close to the tar-sampling connection (Figure 1). Thus, the process gas temperature in this place, shown in Figure 4c, is the temperature at which the tar was sampled.

The temperatures of the process gas at the inlet to the scrubber were not high, ranging from 90–110 °C. At the outlet, the temperatures were approximately 30 °C lower (Figure 4c). Under these conditions (low temperature, atmospheric pressure, and no catalyst), the components of the process gas no longer reacted with each other or with the water vapour. The lowest temperature at which the components of the process gas could react with each other was approximately 180 °C, and refers to the process of producing water gas from water vapour and carbon monoxide (see Equation (2)). Therefore, without much error, it

can be assumed that the composition of the process gas at the outlet of the installation was the same as at the tar sampling site.

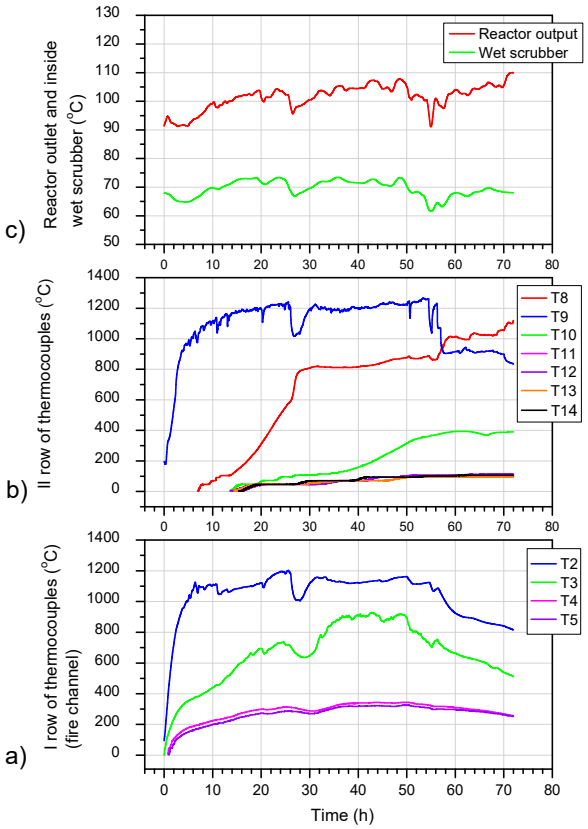

Figure 4. Temperature diagrams [48]: (**a**) row I of thermocouples (fire channel), (**b**) row II of thermocouples, and (**c**) reactor outlet and wet scrubber.

The component of the BTEX group with the lowest boiling point was benzene at 80.1 °C. The other compounds of this group, namely toluene, ethylbenzene, and xylenes, had boiling temperatures of 110.6 °C, 136 °C, and 139 °C, respectively. These temperatures were very close to the temperatures that occurred at the outlet of the reactor and the tar sampling point, so it can be expected that BTEX compounds, which are the lightest components of tar, should be present in the tested samples.

3.3. Process Gas Flow, Composition and Mass Flow of Its Components

Figure 5a shows the process gas flow rate, and Figure 5b,c show the composition and the mass flow of the individual gas components. The data obtained in Figure 5a show that, from the beginning of the process until approximately 46 h, the flow of the gas received was relatively stable and was in the range of 10–14 m^3/h. After 46 h of the process, the amount of gas produced began to increase, reaching a value of approximately 18 m^3/h. The total amount of the gas produced was 896.94 m^3, with an average flow of 12.46 m^3/h.

The data presented in Figure 5b show that the composition of the produced gas was quite stable throughout the gasification process. Between 25 and 28 h into the process, and after approximately 46 h of the process, a significant decrease in the carbon dioxide content was observed, along with a simultaneous increase in the hydrogen, carbon monoxide, and ethane contents. After approximately 46 h of gasification, the methane content started to gradually increase, and after 60 h, it stabilised at the level of approximately 5%. The methane concentration during the whole process was in the range of 2–5.6%, while the ethane and hydrogen sulfide contents were practically below 0.5% and 0.2%, respectively. Throughout the whole experiment, high concentrations of hydrogen (23–38%) and carbon monoxide (27–46%) were observed.

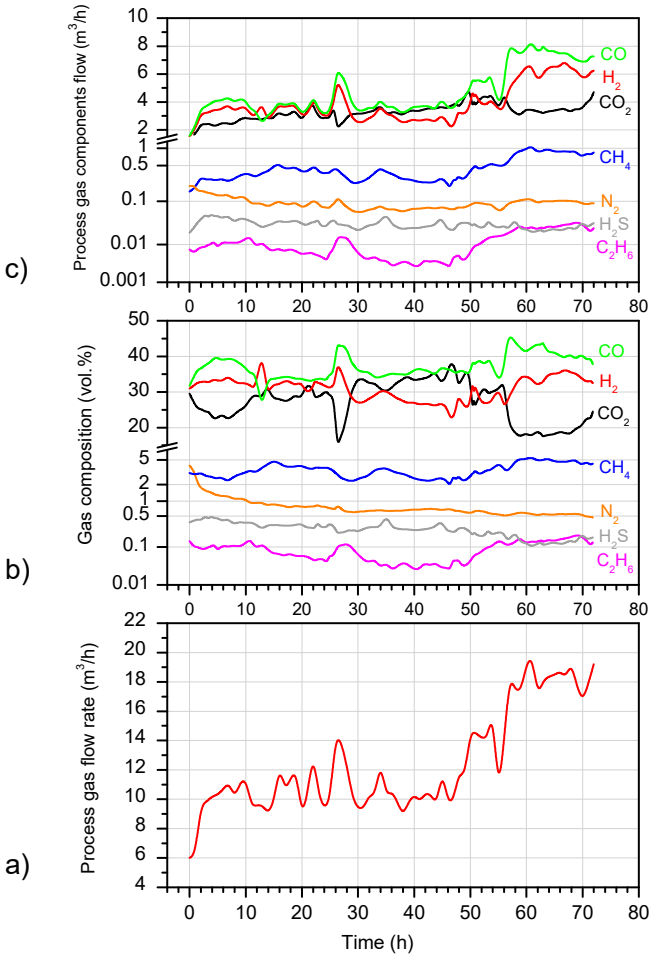

Figure 5. Results for process gas [48]: (**a**) flow rate, (**b**) composition, and (**c**) flow of gas components.

Figure 5c shows that the flow of the hydrogen and carbon monoxide increased twice: it doubled between 25–28 h, as well as from 46 h to the end of the gasification process. In the case of the ethane, its flow rate doubled for the time period of 25–28 h, and from 46 h, the flow even tripled. In the second half of the gasification process, a clear increase in the methane flow was observed. From approximately 46 h to the end of the gasification, the flow of the methane increased to triple its value, and this occurred in the same period of time as the increased flow of the hydrogen and carbon monoxide. Based on the data on the balance of the coal contained in the coal seam before gasification and in the obtained gases, it was possible to calculate the amount of gasified coal. These calculations showed that 532.80 kg of coal was gasified, which constituted 23.17% of the total amount of the raw coal placed in the reactor.

3.4. Pressure Profiles

The course of the pressure changes during the gasification is shown in Figure 6. The presented data show that, in relation to the atmospheric pressure, the gasification process was carried out at a slight overpressure between 0–17 hPa. As there was no negative pressure in the reactor during the coal gasification, the process gas and tar emission were not forced by the suction fan. From the pressure graph (Figure 6), it can be seen that the scrubber had a higher pressure than the reactor outlet; it is also seen that the pressure changes in the scrubber were proportional to the pressure changes at the reactor outlet. The higher pressure in the scrubber was caused by the increase in the amount of water vapour, which was formed as a result of the evaporation of the water that was injected into the scrubber.

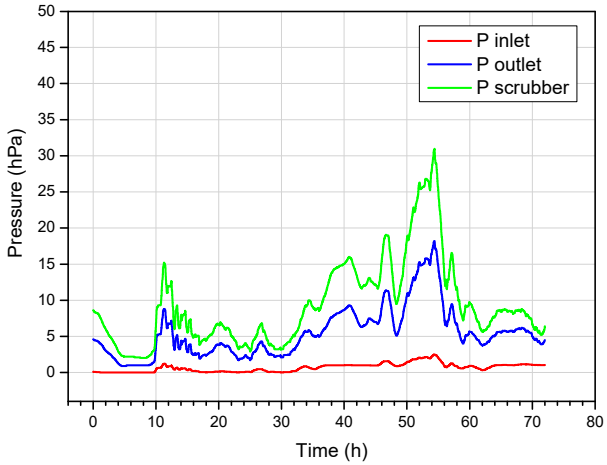

Figure 6. Pressures at reactor inlet, outlet, and inside scrubber [48].

3.5. The Obtained Amount of Postprocessing Water

The total amount of the water taken from the scrubber was 1529 kg. The real amount of the water obtained from the coal gasification was lower, because the water that was added to the wet scrubber to cool the process gas must be subtracted from this amount. The amount of water that was added was 1008 kg, so the postprocess water yield was 521 kg. The gasified block of coal contained only 108.1 kg of water, so the separated water must have originated mainly from the evaporation of the moisture contained in the wet sand, and only some of it would have come from the water contained in the coal. The dependence of the amount of the obtained post-process water (after subtracting the water that was added to the scrubber) on the gasification time is shown in Figure 7.

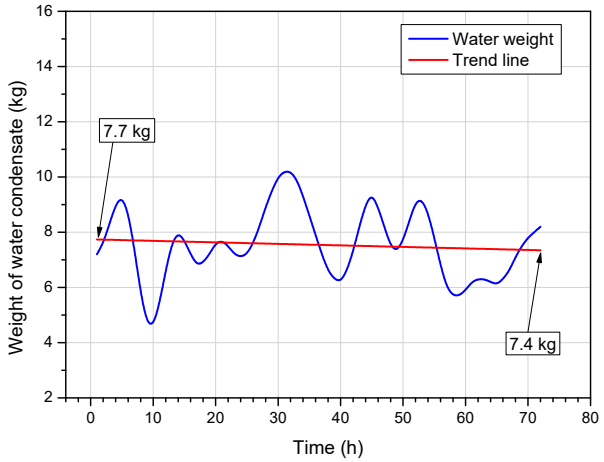

Figure 7. Weight of water condensate [48].

The lowest and highest amounts of the water produced, amounting to 4.7 kg and 10.2 kg, were recorded at 10 and 31 h of the process, respectively. The trend line for the changes in the amount of obtained water, shown in Figure 7, has a downwards trend, which indicates that, as the gasification progressed, the amount of water that was released decreased.

3.6. Concentration and Mass Flow of BTEX, PAHs and Phenols in Tar

The concentrations of the individual tar components are shown in Figures 8–10, while the total list of the analysed compounds and their average concentrations are shown in Table 4.

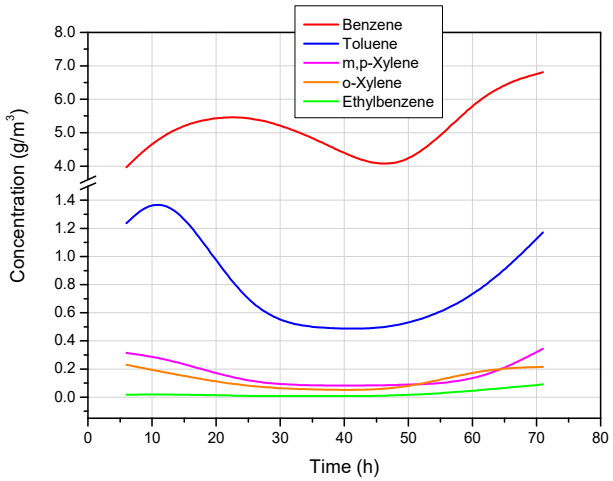

Figure 8. The concentration of BTEX components.

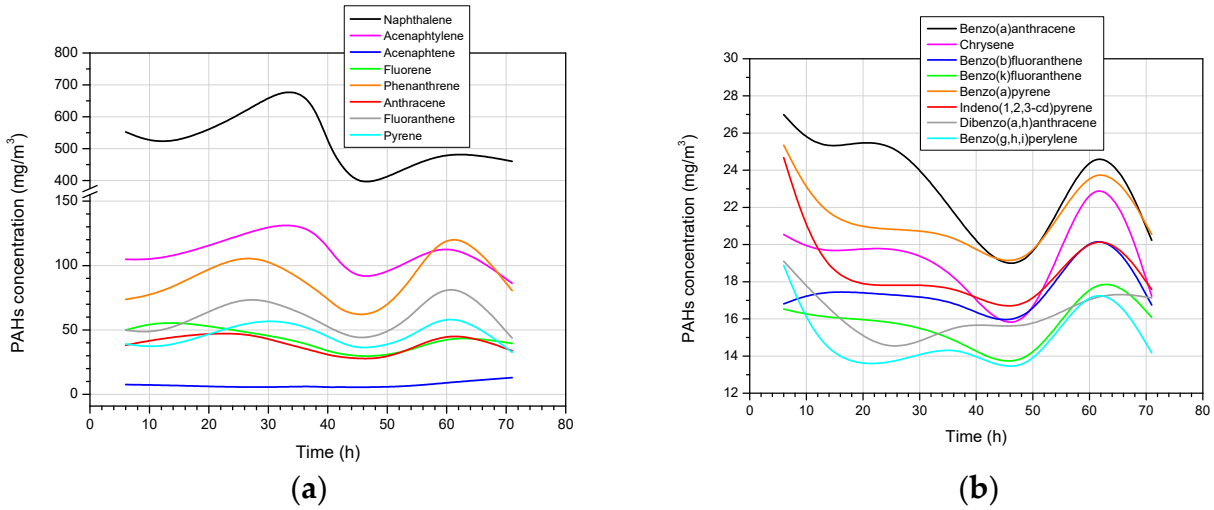

Figure 9. (**a**) The concentration of PAH components with high concentration. (**b**) The concentration of PAH components with low concentration.

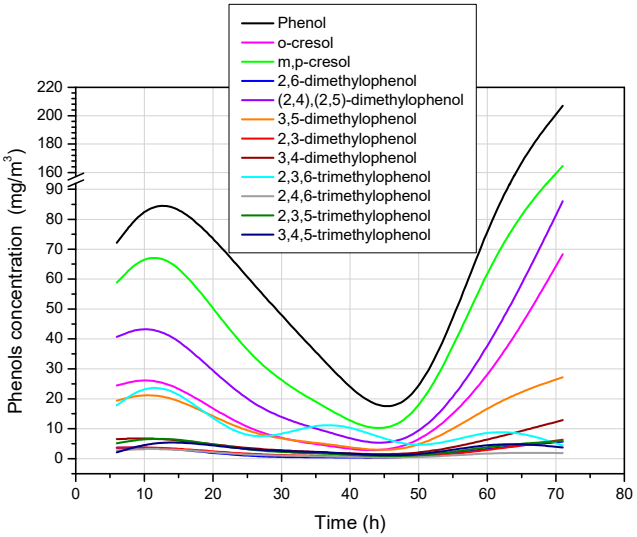

Figure 10. The concentration of phenols.

Table 4. List of analysed hydrocarbons and their average concentrations.

No.	Compounds	Average Concentration (mg/m^3)	Molar Mass (g/mol)
	BTEX		
1	Benzene	5051.2	78.11
2	Toluene	708.6	92.14
3	m,p-Xylene	148.7	106.17
4	o-Xylene	103.1	106.17
5	Ethylbenzene	23.3	106.17
	Total BTEX	6035.0	
	PAHs		
1	Naphthalene	522.9	128.17
2	Acenaphtylene	110.7	152.19
3	Acenaphtene	7.2	154.21
4	Fluorene	43.3	166.22
5	Phenanthrene	91.6	178.23
6	Anthracene	39.8	178.23
7	Fluoranthene	61.7	202.25
8	Pyrene	47.0	202.25
9	Benzo(a)anthracene	23.2	228.29
10	Chryzene	19.3	228.29
11	Benzo(b)fluoranthene	17.6	252.31
12	Benzo(k)fluoranthene	15.8	252.31
13	Benzo(a)pyrene	21.3	252.31
14	Indenol(1,2,3-cd)pyrene	18.4	276.33
15	Dibenzo(a,h)anthracene	16.1	278.35
16	Benzo(g,h,i)perylene	14.8	276.33
	Total PAHs	1070.7	
	Phenols		
1	Phenol	69.1	94.11
2	o-cresol	17.8	108.14
3	m,p-cresol	48.2	108.14
4	2,6-dimethylophenol	2.0	122.16
5	(2,4),(2,5)-dimethylophenol	26.9	122.16
6	3,5-dimethylophenol	12.2	122.16
7	2,3-dimethylophenol	2.2	122.16
8	3,4- dimethylophenol	4.6	122.16
9	2,3,6-trimethylophenol	10.8	136.19
10	2,4,6-trimethylophenol	1.5	136.19
11	2,3,5-trimethylophenol	3.4	136.19
12	3,4,5-trimethylophenol	3.4	136.19
	Total Phenols	202.1	

Figure 8 shows that the concentration of benzene was the highest among all the hydrocarbons of the BTEX group, amounting to an average of 5051.2 mg/m^3. The next most concentrated compound was toluene, with an average concentration of 708.6 mg/m^3. The average concentrations of the other BTEX components (m,p-xylene, o-xylene, and ethylbenzene) were significantly lower, and amounted to 148.7, 103.1, and 23.3 mg/m^3, respectively.

Figure 9a,b show the concentrations of the PAH compounds at high and low concentrations. The highest concentration of this group of compounds was characterised by naphthalene, acenaphtylene, and phenanthrene. Their average concentrations in the process gas were 522.9, 110.7, and 91.6 mg/m^3, respectively.

Phenols, whose concentrations are shown in Figure 10, are the third group of the compounds that were tested. In this group of compounds, the highest average concentration was characterised by phenol (69.1 mg/m^3), followed in decreasing order by m,p-cresol (48.2 mg/m^3) and (2,4),(2,5)-dimethylphenol (26.9 mg/m^3). The concentrations of the remaining compounds in this group were significantly lower (Table 4).

3.7. Concentrations, Mass Flows and Proportion of the Sum of BTEX, PAH and Phenol Compounds

Based on the results that were obtained, the concentrations of the individual compounds in the groups were summed and presented as total concentrations of the BTEX, PAHs, and phenols. The mass flow of these groups in the process gas and their mutual proportions were also calculated. The results that were obtained are presented in Figure 11a–c.

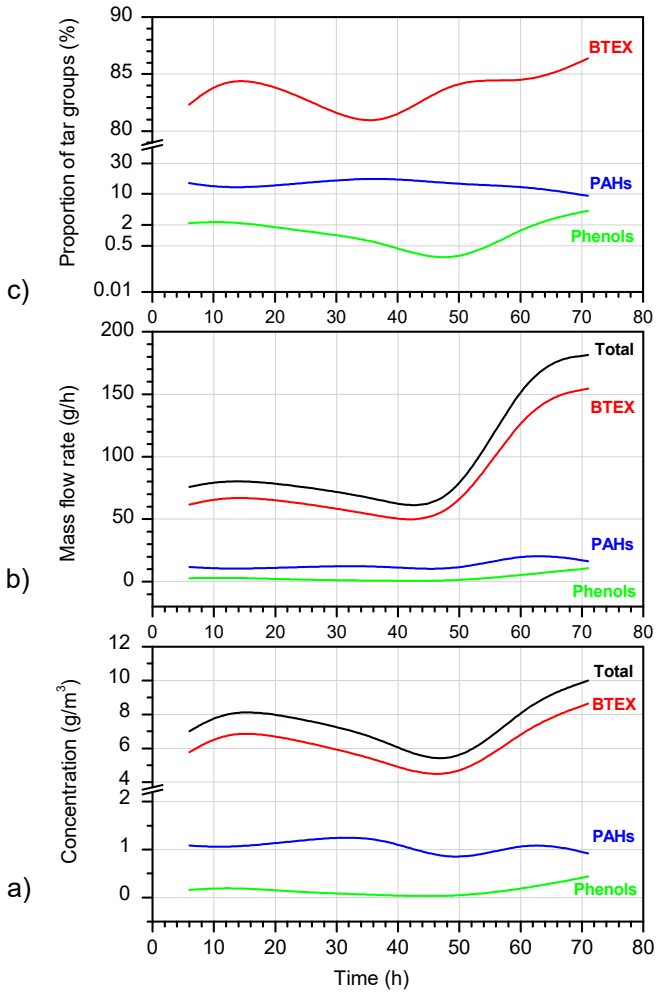

Figure 11. Results for the total sum of BTEX, PAHs, and phenol compounds: (**a**) concentration, (**b**) mass flow rate, and (**c**) proportion of tar groups.

3.7.1. Concentration of Tar Groups

Figure 11a shows that, after the ignition of the coal seam, the BTEX concentrations started to increase from a value of approximately 5.7 g/m^3, and then started to decrease to a minimum value of 3.7 g/m^3 at the 46th hour of the process. After that, the BTEX concentrations increased again to a final value of 8.60 g/m^3. The second group of the compounds, in terms of mass, are the PAHs. At the beginning of the experiment, the PAH concentrations decreased slightly, then started to increase until hour 30, and then decreased again until hour 46. Thereafter, their concentrations increased again, and after hour 60, they decreased again until the end of the gasification process. At the start of the gasification, the PAH concentration was 1.08 g/m^3, and at the end, the concentration was 0.93 g/m^3 (average 1.07 g/m^3). Phenols were the group of compounds whose obtained amount was the lowest. At the beginning of the process, the concentration of the phenols was 0.15 g/m^3, and after a temporary increase, it dropped to 0.033 g/m^3. Thereafter, a steady increase in the concentration was recorded up to a maximum value of 0.45 g/m^3 at

the end of the gasification test. The average concentration of the phenols in the process gas was 0.20 g/m^3.

3.7.2. Mass Flows and Proportion of Tar Groups

From the graphs of the mass flows of the BTEX, PAHs, and phenols, as shown in Figure 11b, it can be seen that, up to approximately 46 h of the process, the curves are similar in shape to the curves that show the changes of their respective concentrations in the process gas (Figure 11a). After 46 h of the process, a large increase in the mass flow rates of all the tested tar groups was observed. With regard to the changes in the proportions of the discussed groups of compounds, Figure 11c shows that, after the ignition of the coal seam, the percentage of the BTEX compounds, which were the dominant group in the tar up to the 15th hour of the process, increased from 82% to 84%, and then started to decrease to a minimum value of 81% at the 46th hour of the process. Starting at 46 h, the proportion of the BTEX in the tar was observed to increase to a final value of 86%. As shown in Figure 11c, the proportions of the PAH and phenol compounds were significantly lower than the proportion of the BTEX compounds. The proportion of the PAH compounds up to the 15th hour of gasification, initially amounting to 16%, dropped to 13%. By the 46th hour, there was an increase to approximately 17%, followed by a decrease to 9% at the end of the experiment. In approximately the first 46 h, the proportion of the phenols decreased in the range of 2–0.1%, and then constantly increased to the final value of 4%.

3.8. Residence Time of the Tar in the Reactor

The residence time of the tar vapours in the reactor can be calculated based on the temperatures in the reactor, the geometry of the reactor, and the amount of gases and water released in the process. The volumes of the tar vapours were neglected in the calculations, because they constituted 0.05–0.15% of the combined volumes of the produced gases and water vapour. The results of the calculations are presented in Figure 12.

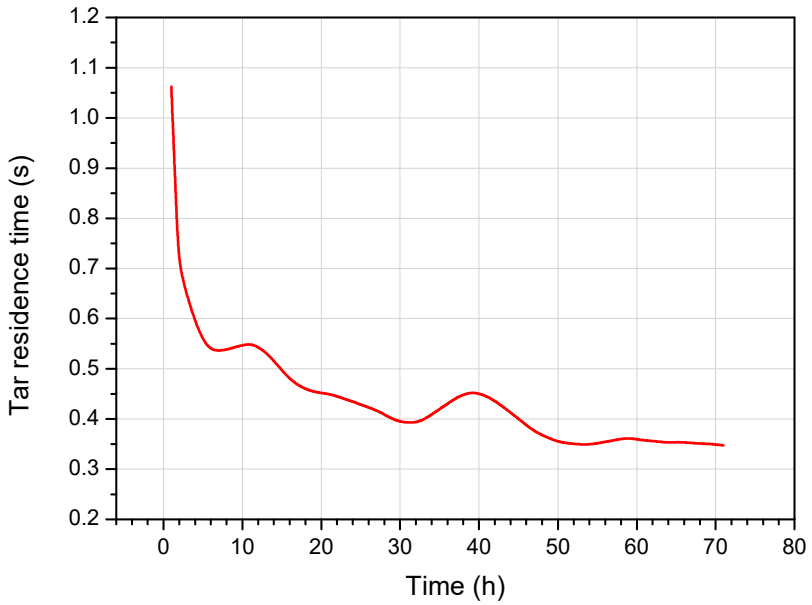

Figure 12. Residence time of tar inside the reactor.

Figure 12 shows that, at the beginning of the experiment, the residence time of the tar in the reactor was approximately 1 s, and at the end, it was 0.35 s. This means that there was a threefold decrease as the reaction progressed. The visible local increases in the residence time at approximately 10 h and 40 h of the process are due to the lower amount of water released at these times (Figure 7).

3.9. Molar Masses and H/C Ratio in Tar

Based on the data on the yields of the analysed components of the tar and their molecular weights, graphs of their changes in molar mass and H/C ratio during the gasification process were prepared. The results of the calculations are presented in Figure 13.

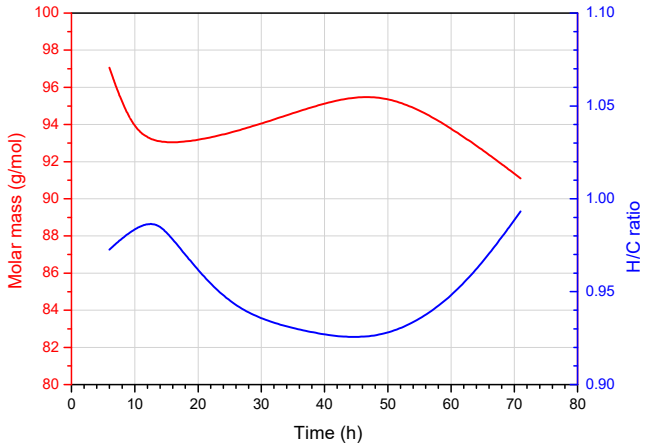

Figure 13. Molar mass of tar and H/C ratio.

Figure 13 shows that the changes in molar mass and H/C ratio were inversely proportional to each other. An increase in the molecular weight of the tar corresponded to a decrease in the H/C ratio, and vice versa. This validates the analysis and calculations, because the lighter the tar was, the higher the H/C ratio. Figure 13 shows that, at the beginning of the process until approximately 15 h, the molar mass of the tar decreased from a value of approximately 97 g/mol to 93 g/mol. At the same time, the H/C ratio increased from 0.97 to 0.99. Then, by the 46th hour, the molar mass began to increase, and the H/C ratio began to decrease. At the 46th hour of the process, the molar mass was 95.5 g/mol and the H/C ratio was 0.93. From this point in time until the end of the experiment, the molar mass began to decrease to a value of 91.1 g/mol, and the H/C ratio steadily increased to a final value of 0.99.

3.10. Total Production of BTEX, PAHs and Phenols

The total production of the particular compounds in the tar was calculated based on the data for the amount of gas that was produced and the data for the concentrations of those compounds. The results are presented in Figure 14.

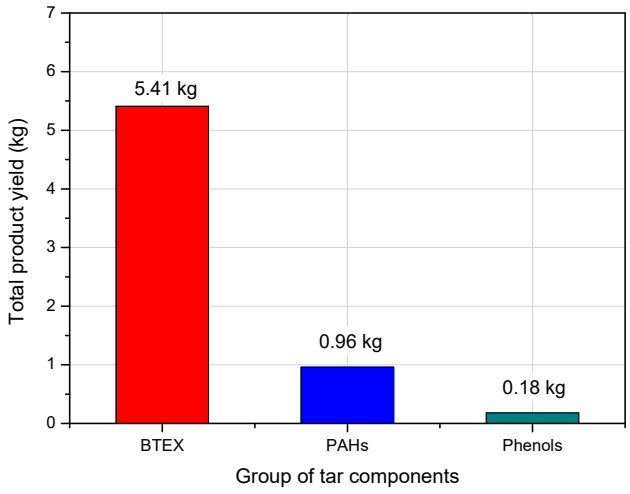

Figure 14. Total production of BTEX, PAH, and phenol compounds.

The calculations show that, during the coal gasification test, the amounts of the BTEX, PAHs, and phenols that were produced were 5.41 kg, 0.96 kg, and 0.18 kg, respectively. Their average concentrations were 82.6%, 14.7%, and 2.7%, respectively. The total mass of these compounds was 6.55 kg. An inspection of the internal sections of the process gas pipeline following the process did not reveal any tar deposits on the walls, which indicates that practically all of the tar produced during the gasification was transported outside the reactor in the gas stream. An estimation of the efficiency of the tar production from the gasified coal was made, taking into account the total amount of the gasified coal, which was 532.8 kg. The tar yield was 12.3 kg per ton of coal, which accounted for 1.23% of the total mass of the gasified coal. This is not the summary amount of the tar produced, because only a part of the compounds present in the tar was determined, so the total yield should be higher.

3.11. Measurement Errors

During each experiment, measurement errors are made, the magnitude of which depends on the accuracy of the analytical methods that are used, the accuracy of the measuring apparatus, the methodology that is used to conduct the experiment, and the sampling used for the analysis. It is assumed that the possible inaccuracies of the results presented in this work result from the imprecise determination of hydrocarbon concentrations in tar samples taken into sorption tubes. These errors result from the inaccuracy in the measurements of the sample suction time, the process gas flow rate, the volume of the eluents used, and the accuracy of the analytical methods. The total assay error can be estimated to be up to $\pm$20% of the measured value, depending on the measured concentration level. The estimation of the amount of tar that was obtained is also flawed, because it was based on the analysis of 33 specific compounds (from the BTEX, phenol, and PAH groups), while the actual number of the chemical compounds that have been identified in tar is much higher, and amounts to several thousand. The content of many of these compounds in tar does not even exceed 1%. The estimation of this error was carried out using a semiquantitative method by analysing the spectra of the samples obtained during the chromatographic analysis that was performed in scanning mode. For this purpose, the ratio (in percentage) was calculated from the area of the peaks corresponding to the analysed compounds, divided by the sum of the areas of all the peaks obtained in the spectrum. Due to their very large number, those with a percentage share of less than 0.1% were omitted. The error that was calculated on this basis was approximately (minus) 30% of the total tar mass. In connection with the error in the tar composition measurements, the errors in the molecular weight of the tar and the H/C ratio are also estimated to not exceed 30%. The maximum measurement errors concerning the other measured physicochemical quantities are not as significant as those in the case of tar. For example, the measurement error for the process gas flow rate was approximately $\pm$0.01 dm^3, the temperature error was $\pm$1 °C, and the gas concentration error was $\pm$0.02 vol. %.

4. Discussion of the Results Obtained

The presented data show that, during the gasification test, tar products were constantly present in the process gases. This is because, during the process, the gasification zone was expanding, which meant that subsequent amounts of coal were gasified, producing new amounts of tar. Taking into account that tar formation stops when the temperature exceeds approximately 1000 °C, the tar was formed in areas where the temperature was lower than that. The gasification time interval was very important, starting from approximately hour 46 of the process, until the end of the process. During this time, the process gas stream started to increase, and at the same time, the concentrations of the hydrogen, methane, ethane, and carbon monoxide also started to increase. At the same time, in the process gas, the concentration of the sum of the compounds from the BTEX group almost doubled, and the flux of those compounds tripled. Similar changes were recorded in the proportions of the individual compounds. There was an increase in the proportions of the

BTEX compounds and phenol compounds, and a decrease in the proportion of the PAH compounds. The data show that the changes in the process gas and the tested tar were influenced by the water that was contained in the wet sand that surrounded the gasified coal seam. After the ignition of the coal, the temperature rapidly increased around the location of the igniting charge. The tar started to rise from the coal, and the water started to evaporate from the sand upon which the block of coal had been placed. The water vapour gradually reacted with the coal, and, as a result, high concentrations of hydrogen and carbon monoxide were observed in the resulting gases. From the moment of ignition until approximately the 15th hour of the process, the amount of light BTEX fractions increased in the emitted tar. Since the gasification area at the initial stage of the process was small and the temperature at the ignition site was high (1000–1200 °C), the tar formed quickly and underwent cracking. These tar cracking processes were favoured by the long residence time of the tar in the reactor during this period of time. As a result of the cracking, the molecular weight of the tar decreased, and the H/C ratio increased. After 15 h of the process, as the gasification progressed, the gasification zone continued to expand, and the amount of released water stabilised. Between 15 and 46 h of the process, the amount of tar that was produced decreased, as much of it was released earlier. At this time, the heavier components of the tar were released from the coal, which changed their composition due to the intensification of the secondary processes taking place under the influence of the rapidly rising temperature. In the produced tar, the concentrations of the BTEX and phenol compounds decreased, while the concentration of the PAH compounds increased, and then decreased again between 15–34 h. As a result, the molecular weight of the tar increased, and the H/C ratio was lowered. From the 46th hour to the end of the gasification process, a significant increase in the amount of process gas produced was observed. This was most likely the result of the gasification zone moving closer to the wet sand. Due to the high temperature, a large amount of water vapour began to escape from the sand and reacted with the incandescent coal. As a result, large amounts of hydrogen and carbon monoxide were produced.

Simultaneously, the reaction of steam with the coal-exposed "fresh" portions of the coal allowed for additional large amounts of tar to start escaping. The explanation for the large increase in the BTEX yields following the 46th hour of the process is more complex, because, according to theory, there could have been two reaction mechanisms that complemented each other. According to the first mechanism, at higher temperatures, the presence of steam increases the rate of the decomposition of the heavier components of the tar (cracking), resulting in an increase in its yield and a decrease in its molecular weight. According to the second mechanism, at lower temperatures, the hydrogen that is generated can reform into the separated tar components and inhibit the repolymerisation reaction of their molecules. As a result of both reactions, the amount of lighter separated tar increases. It seems that, under the conditions prevailing in the reactor (a high temperature at the beginning and a lower temperature at the end, and the presence of hydrogen and steam), apart from cracking, some reforming processes (isomerisation, cyclization, and aromatisation) could have taken place. As a result, the amount of the BTEX group hydrocarbons that formed was high. From the temperature data presented, the temperature in the reactor could have been in the range of 600–1200 °C. This suggests that the high-temperature mechanism, i.e., the cracking of the heavier components of the tar in the presence of hydrogen, is responsible for the high amount of the tar released from 46 h until the end of the process.

The amount of postprocess water that was obtained from this process was 521 kg. The conversion of this quantity of liquid water into steam requires supplying approximately 1265 MJ of thermal energy, which is equivalent to the combustion of approximately 56 kg of gasified coal. The consumption of this amount of energy must have lowered the temperature in the reactor, as shown in the temperature diagrams. The curves of the temperature changes that are presented in Figure 4a,b show that, from a certain point, the rate of the temperature increase in the gasified bed decreased, or even stopped, which confirms the influence of water evaporation on the change in the process temperatures.

The yield of the tar that was obtained, in terms of the amount of the gasified coal, was approximately 1.23% of the mass of the raw coal that was gasified. Taking into account a 30% error in underestimating the amount of tar that was obtained, it was calculated that the yield of the tar in this process was approximately 1.8% of the mass of the gasified coal. When comparing the tar yield from the UCG process with the tar yield from a classic coal coking process, it should be taken into account that the coke oven tar yield is approximately 3.5–5% of the weight of the coked coal. This is the efficiency without light fractions (mainly BTEX compounds), as these fractions are separated from the coke oven gas as crude benzole. The yield of the crude benzol is typically 1.1% of the weight of the coked coal. Together with the crude benzole, the yield of the coke oven tar is 4.6–6.1%. This means that the tar yield from the UCG process was approximately 2.5–3.3 (3x on average) times lower than that of the coke oven tar. The tar from the UCG process contained 82.6% of BTEX compounds, 14.7% of PAH compounds, and 2.7% of phenol compounds. The yield of the benzene is very high, amounting to 0.95 kg/ton of the gasified coal, which is comparable to the yield of the benzene produced in the coal coking process, amounting to approximately 1 kg/ton. The high average content of the benzene in the tested tar (77.1%) indicates that it was formed as a result of thermal cracking. Starting from the 46th hour of the process, an increase in the amount of ethane produced is also visible. As ethane is released during the cracking of the tar, the increase in ethane during these time intervals indicates the occurrence of cracking processes in the tar produced. Figure 5b shows that, at approximately the 25th hour of the process, there was also a temporary increase in the concentration of the ethane, carbon monoxide, and hydrogen. This was probably due to a momentary release of water vapour, which caused exactly the same phenomena in the process gas and the tar, and occurred from hour 46 onwards. The cracking and reforming of the tar also produces methane and hydrogen. These compounds increase the concentrations of the flammable components of the process gas, but in the UCG process, their main source is the reaction of steam with the coal.

In discussing the results obtained, it should also be taken into account that the iron contained in siderite may have had a catalytic effect in the Bouduard reaction. This could be possible if this iron was dispersed in the gasified coal. In this experiment, the siderite was arranged in a thick, solid layer, so the catalytic action, if it did occur, was only to a small extent and had no effect on the obtained results.

The results of the ex situ coal gasification presented in the article show that, during this process, tar was released with different intensities, and its efficiency and composition depended on the gasification parameters. Under in situ conditions, tar will also be released, because the process of its formation results from the chemistry of phenomena occurring during coal pyrolysis.

A review of the literature shows that the presence of tar in the process gas causes numerous problems related to its condensation in the pipelines that transport the produced gas to the surface. Knowledge of the yield and composition of the produced tar, determined on the basis of measurements that were made directly from the reactor outlet, is very important, because such data can minimize the adverse effects associated with the presence of tar in the process gas to an acceptable minimum. The ex situ coal gasification studies presented in the article were aimed at identifying this problem to a significant extent.

5. Conclusions

(1) The moisture content in the surroundings of the gasified block of coal had a significant impact on the gasification process, because the water reacted with the glowing coal and produced large amounts of process gas that was rich in hydrogen and carbon monoxide. This result indicates that the participation of water in the UCG process is necessary, and plays an important role.

(2) The steam generated, in addition to producing process gas components, stimulated the release of tar from the gasified coal. At high temperatures in the reactor, in the presence of hydrogen and steam, this tar could undergo hydrocracking and steam

reforming. As a result of these processes, the tar has a low molecular weight and a high H/C ratio.

(3) The increased emission of ethane, observed particularly in the second half of the test, was most probably a result of the hydrocracking and steam reforming processes of the heavier tar fragments.

(4) The obtained tar contained 82.6% of BTEX compounds, 14.7% of PAH compounds, and 2.7% of phenol compounds. The very high benzene content, both in the BTEX group and in the whole tar, confirms the occurrence of thermal cracking processes.

(5) The short residence time of the tar in the reactor, approximately 1 s initially and 0.35 s at the end of the gasification, was the result of an increase in the amount of released gas and steam, as well as the appropriately selected parameters of the suction fan operation.

(6) Taking into account measurement errors, the estimated total tar yield from the UCG test that was carried out under atmospheric pressure was approximately 1.8% of the weight of the gasified coal. This value is approximately three times lower than the tar yield from a typical high-temperature coal coking process.

Funding: The research presented in this article was performed within the work "Conducting an ex situ experiment of underground coal gasification with a mineral interlayer" commissioned and funded by the Silesian University of Technology in Gliwice, Department of Applied Geology by order sign ZP/018521/18/ZZ/01987/18.

Data Availability Statement: Not applicable.

Conflicts of Interest: The author declares no conflict of interest or personal relationships that could have appeared to influence the work reported in this paper.

References

1. Atkins. *Underground Coal Gasification—Evidence Statement of Global Warming Potential DECC*; Version 7; Atkins: Epsom, UK, 2015; p. 5142635.
2. Ladner, W.R. The products of coal pyrolysis: Properties, conversion and reactivity. *Fuel Process.* **1988**, *20*, 207–222. [CrossRef]
3. Perkins, G.; Toit, E.; Cochrane, G.; Bollaert, G. Overview of underground coal gasification operations at Chinchilla, Australia. *Energy Sources Part A Recovery Util. Environ. Eff.* **2016**, *38*, 3639–3646. [CrossRef]
4. Pirard, J.P.; Brasseur, A.; Coëme, A.; Mostade, M.; Pirlot, P. Results of tracer test during the El Tremedal underground coal gasification at great depth. *Fuel* **2000**, *79*, 471–478. [CrossRef]
5. Wang, G.X.; Wang, Z.T.; Feng, B.; Rudolph, V.; Jiao, L. Semi-industrial tests on enhanced underground coal gasification at Zhong-Liang-Shan coal mine. *Asia Pac. J. Chem Eng.* **2009**, *4*, 771–779. [CrossRef]
6. Kaiser, M.; Wanzl, W. Characterization And Comparison Of Liquid Products From Coal Pyrolysis In Laboratory And Process Development Units. *Fuel Process. Technol.* **1988**, *20*, 23–32. [CrossRef]
7. Karabon, B. *Smoła Węglowa i Benzol Koksowniczy Jako Surowce Przemysłu Chemicznego*; Oficyna Wydawnicza Politechniki Wrocławskiej: Wrocław, Poland, 2002. (In Polish)
8. Škvareková, E.; Wittenberger, G.; Šofranko, M. Tar related issues in underground coal gasification. *Acta Montan. Slovaca* **2016**, *21*, 298–305.
9. Wiatowski, M.; Kapusta, K. Evolution of tar compound in raw gas from a pilot-scale underground coal gasification (UCG) trial at Wieczorek mine in Poland. *Fuel* **2020**, *276*, 118070. [CrossRef]
10. Basu, P. *Combustion and Gasification in Fluidized Beds*; CRC Press: Boca Raton, FL, USA, 2006; 496p, ISBN 0-8493-3396-2.
11. Dermot, J.R. A syngas network for reducing industrial carbon footprint and energy use. *Appl. Therm. Eng.* **2013**, *53*, 299–304.
12. Porada, S.; Czerski, G.; Dziok, T.; Grzywacz, P.; Makowska, D. Kinetics of steam gasification of bituminous coals in terms of their use for underground coal gasification. *Fuel Process. Technol.* **2015**, *130*, 282–291. [CrossRef]
13. Byron Smith, R.J.; Muruganandam, L.; Murthy, S.S.H. A Review of the Water Gas Shift Reaction Kinetics. *Int. J. Chem. React. Eng.* **2010**, *8*, 1–39.
14. Vreugdenhil, B.J.; Zwart, R.W.R. *Tar Formation in Pyrolysis and Gasification: ECN Biomass, Coal and Environmental Research*; ECN Report Number: ECN-E-08-087; ECN: Petten, The Netherlans, 2009; pp. 1–37.
15. Wang, Z.; Liang, D.; Li, Y.; Tian, H.; Liang, J. Pyrolysis characteristics of large-scale bituminous coal. *J. Anal. Appl. Pyrolysis* **2021**, *158*, 105060. [CrossRef]
16. Xi, J.; Linag, J.; Sheng, X.; Shi, L.; Li, S. Characteristics of lump lignite pyrolysis and the influence of temperature on lignite swelling in underground coal gasification. *J. Anal. Appl. Pyrolysis* **2016**, *117*, 228–235. [CrossRef]

17. Zhang, H.R.; Li, S.; Kelly, K.E.; Eddings, E.G. Underground in situ coal thermal treatment for synthetic fuels production. *Prog. Energy Combust. Sci.* **2017**, *62*, 1–32. [CrossRef]
18. Hu, E.; Zeng, X.; Ma, D.; Wang, F.; Yi, X.; Li, Y.; Fu, X. Effects of Moisture content in Coal on Pyrolysis Behavior in indirectly Heated Fixed-Bed Reactor with Internals. *Energy Fuels* **2017**, *31*, 1347–1354. [CrossRef]
19. Zhang, C.; Wu, R.; Hu, E.; Lis, S.; Xu, G. Coal Pyrolysis for High-Quality Tar and Gas in 100 kg Fixed Bed Enhanced with Internals. *Energy Fuels* **2014**, *28*, 7294–7302. [CrossRef]
20. Korus, A.; Samson, A.; Szlęk, A.; Katelbach-Woźniak, A.; Sładek, S. Pyrolytic toluene conversion to benzene and coke over activated carbon in a fixed-bed reactor. *Fuel* **2017**, *207*, 283–292. [CrossRef]
21. Kim, Y.K.; Park, J.I.; Jung, D.; Miyawaki, J.; Yoon, S.H.; Mochida, I. Low-temperature catalytic conversion of lignite: 3. Tar reforming using the supported potassium carbonate. *J. Ind. Eng. Chem.* **2014**, *20*, 9–12.
22. Ashok, J.; Kawi, S. Nickel−Iron Alloy Supported over Iron−Alumina Catalysts for Steam Reforming of Biomass Tar Model Compound. *ACS Catal.* **2014**, *4*, 289–301. [CrossRef]
23. Miura, K.; Kawase, M.; Nakagawa, H.; Ashida, R.; Nakai, T. Conversion of Tar in Hot Coke Oven Gas by Pyrolysis and Steam Reforming. *J. Chem. Eng. Jpn.* **2003**, *36*, 735–741. [CrossRef]
24. Paasen, S.V.B.; Kiel, J.H.A. *Tar Formation in a Fluidised Bed Gasifier: Impact of Fuel Properties and Operating Conditions*; ECN-C-04-13; ECN: Petten, The Netherlans, 2004.
25. Klebingat, S.; Kempka, T.; Schulten, M.; Azzam, R.; Manuel Fernández-Steeger, T.M. Innovative hermodynamic underground coal gasification model for coupled synthesis gas quality and tar production analyses. *Fuel* **2016**, *183*, 680–686. [CrossRef]
26. Campbell, G.G.; Brandenburg, C.F.; Boyd, R.M. *Preliminary Evaluation of Underground Coal Gasification at Hanna, Wyoming*; Technical Progress Report 82; US Department of the Interior, Bureau of Mines Coal Gasification Program: Harrisburg, PA, USA, 1974.
27. Hill, R.W.; Thorsness, C.B.; Cena, R.J.; Stephens, D.R. Results of the Centralia underground coal gasification field test. In Proceedings of the 10th Annual Underground Coal Gasification Symposium, DOE/METC-85/5, Williamsburg, VA, USA, 12–15 August 1984; pp. 11–26.
28. Klebingat, S.; Kempka, T.; Schulten, M.; Azzam, R.; Manuel Fernández-Steeger, T.M. Optimization of synthesis gas heating values and tar by-product yield in underground coal gasification. *Fuel* **2018**, *229*, 248–269. [CrossRef]
29. Klebingat, S. Development, Validation and Scenario Analyses of Two Underground Coal Gasification (UCG) Model Approaches Focussing on Gas Quality-Tar Production Control and Tar Pollutant-Water Solubility Risk Prognoses. Ph.D. Thesis, Rheinisch Westfaelische Technische Hochschule—RWTH Aachen University, Aachen, Germany, 2016. [CrossRef]
30. Camp, D.W. *A Review of Underground Coal Gasification Research and Development in the United States*; LLNL-TR-733952; Lawrence Livermore National Laboratory: Livermore, CA, USA, 2017.
31. Arinenkov, D.M. Apparatus for Opening Ports in Gas Pipes in Underground Gasification of Coal. Russian Patent 64,509, 30 April 1945.
32. Capp, J.P.; Lowe, R.W.; Simon, D.W. *Underground Gasification of Coal, 1945–1960: A Bibliography. U.S. Dept. of the Interior, Bureau of Mines, Information Circular 8193 233 p. 27 cm. (U. S.) 1. Coal Gasification, Underground-Bibl. I. Title. (Series) TN23.un no. 8193 622.06173*; U.S. Deptartmanet of the Interior Library: Washington, DC, USA, 1963.
33. Minister of Fuel and Power (Great Britain). *British Trials in Underground Gasification, 1949–1955*; H.M. Sta. Off.; Ministry of Power: London, UK, 1956; p. 90.
34. Barbour, F.A.; Campbell, S.L.; Covell, J.R. *Analysis of Coal Tars Collected from Rocky Mountain 1 ELW and CRIP Modules*; Technical Report: DOE/MC/II076-2655; U.S. Department of Energy: Washington, DC, USA, 1989.
35. Philips, N.P.; Muela, C.A. *In-Situ Coal Gasification: Status of Technology and Environmental Impact*; U.S. Environmental Protection Agency, Office of Research and Development: Washington, DC, USA, 1977.
36. Perkins, G.; Toit, E.; Koning, B.; Ulbrich, A. Unconventional Oil Production from Underground Coal Gasification and Gas to Liquids Technologies. In Proceedings of the SPE Unconventional Resources Conference and Exhibition-Asia Pacific, Brisbane, Australia, 11–13 November 2013. [CrossRef]
37. Wiatowski, M.; Muzyka, R.; Kapusta, K.; Chrubasik, M. Changes in properties of tar obtained during underground coal gasification process. *Int. J. Coal Sci. Technol.* **2021**, *8*, 1054–1066. [CrossRef]
38. Wiatowski, M.; Kapusta, K.; Stańczyk, K. Analysis and characteristics of tars collected during a pilot-scale underground coal gasification (UCG) trial. *Fuel* **2017**, *208*, 595–601. [CrossRef]
39. Wiatowski, M.; Kapusta, K.; Muzyka, K. Study of properties of tar obtained from coal gasification trials. *Fuel* **2018**, *228*, 206–214. [CrossRef]
40. Pavlovich, L.B.; Strakhov, V.M. Producing Hydrocarbons by the Underground Gasification of Coal. *Coke Chem.* **2013**, *56*, 349–355. [CrossRef]
41. Camp, D.W.; White, J.A. *Underground Coal Gasification: An Overview of Groundwater Contamination Hazards and Mitigation Strategies*; LLNL-TR-668633; Lawrence Livermore National Laboratory: Livermore, CA, USA, 2015.
42. Barbour, F.A.; Cummings, R.E. *Comparison of Coal Tars Generated by Pyrolysis of Hanna Coal and UCG Hanna IVB Coal Tars*; Report Cooperative Agreement No. DE-FC21-83FE60177; Western Research Institute: Laramie, WY, USA, 1986.
43. Barbour, F.A.; Campbell, S.L.; Covell, J.R. *Analysis of Coal Tars Collected from Rocky Mountain 1 ELW AND CRIP Modules*; Report Cooperative Agreement No. DE-FC21-86MC11076; Western Research Institute: Laramie, WY, USA, 1989.
44. Kreinin, E.V.; Revva, M. *Underground Gasification of Coal. Kemerouskoe Knizhnoe Izdatel'stoo*; Report UCRL Trans-10810 (1974); Lawrence Livermore Laboratory: Livermore, CA, USA, 1966.

45. Feng, L.; Dong, M.; Wu, Y.; Gu, J. Comparison of Tar Samples from Reaction Zone and Outlet in Ex-Situ Underground Coal Gasification Experiment. *Energies* **2021**, *14*, 8570. [CrossRef]
46. Dong, M.; Feng, L.; Zhou, Q.; Zhou, S.; Xu, X.; Qin, B. Spatial and temporal evolution of tar during ex-situ underground coal gasification. *Fuel* **2022**, *317*, 123423. [CrossRef]
47. Feng, L.; Liu, J.; Xin, J.; Pang, J. Application of Gas Chromatography Mass Spectrometry in Tar Analysis from Underground Gasification. *Separations* **2023**, *10*, 12. [CrossRef]
48. Wiatowski, M.; Kapusta, K.; Nowak, J.; Szyja, M.; Basa, W. An ex situ underground coal gasification experiment with a siderite interlayer: Course of the process, production gas, temperatures and energy efficiency. *Int. J. Coal Sci. Technol.* **2021**, *8*, 1447–1460. [CrossRef]
49. Hildebrandt, R. Sposób rozruchu georeaktora podziemnego zgazowania węgla. *Wiadomości Górnicze* **2015**, *11*, 593–596. (In Polish)